

Flexible screen printed thick film thermoelectric generator with reduced material resistivity

Z. Cao¹, E. Koukharenko, R.N. Torah, J. Tudor and S.P. Beeby

¹University of Southampton, U.K.

z.cao@soton.ac.uk

Abstract. This work presents a flexible thick-film Bismuth Tellurium/Antimony Tellurium (BiTe/SbTe) thermoelectric generator (TEG) with reduced material resistivity fabricated by screen printing technology. Cold isostatic pressing (CIP) was introduced to lower the resistivity of the printed thermoelectric materials. The Seebeck coefficient (α) and the resistivity (ρ) of printed materials were measured as a function of applied pressure. A prototype TEG with 8 thermocouples was fabricated on flexible polyimide substrate. The dimension of a single printed element was $20\text{ mm} \times 2\text{ mm} \times 78.4\text{ }\mu\text{m}$. The coiled-up prototype produced a voltage of 36.4 mV and a maximum power of 40.3 nW from a temperature gradient of 20 °C.

1. Introduction

Thermoelectric generators (TEGs) can generate electrical voltage and power for autonomous microsystems from a thermal gradient. When there is heat flux along a thermoleg, a voltage will be generated from the thermocouple due to the Seebeck Effect [1]. Compared with other energy harvesting approaches, TEGs could operate in locations that lack of illumination and mechanical movement. For example, most patients or elderly people who would benefit from medical sensor systems are physically inactive in their daily life, making mechanical energy harvesting unsuitable for wearable medical sensors. Thus, flexible TEGs are an attractive approach because of their ability and suitability to power miniature electrical devices for wearable applications [2-3].

Screen printing technology has demonstrated its potential to fabricate TEGs on flexible substrate, e.g., Kapton [4]. Compared with photolithography and electrochemical deposition [5], screen printing is a low-cost process and better suited to large area fabrication, which is essential for practical applications. At room temperature, the Bismuth Tellurium ($\text{Bi}_{1.8}\text{Te}_{3.2}$)/Antimony Tellurium (Sb_2Te_3) based thermocouples have high figure of merit (ZT) values. This makes them potentially attractive for use in the screen printed TEGs [1, 4].

The efficiency of a TEG depends on the Z value of the materials ($Z=\alpha^2/(\rho\cdot\lambda)$, where α is the Seebeck coefficient, ρ is the electrical resistivity, and λ is the thermal conductivity). The printed thick film exhibits a porous structure which increases the electric resistivity and hence decreases the Z value. Cold isostatic pressing (CIP) is an approach that uniformly compresses the material over the entire surface by pressure applied through a hydraulic fluid [6]. The compressed material can be either dry particles or pastes. Figure 1 shows the basic principles of the particles densification process during pressing.

While previous work has demonstrated that the high resistivity of the BiTe and SbTe thick films is the bottle neck that limits the power output of the printed planer TEGs [4], in this paper, CIP has been introduced to densify the printed thick films in order to achieve a lower electric resistivity. The Seebeck coefficients and resistivity of thick film samples after different pressures were measured. Optimization of the printing process was also investigated. A coiled-up planar TEG on Kapton substrate was fully

screen printed based on the optimized printing and pressing process condition. The voltage and power output under different temperature gradients were measured

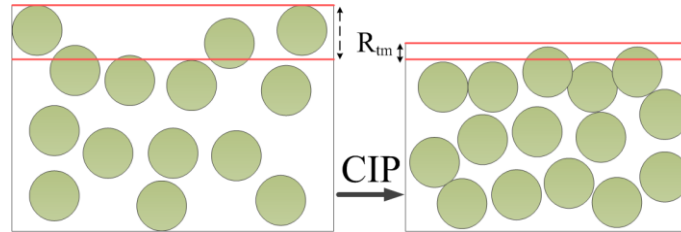


Figure 1. Illustration of particles densification in CIP process

2. Experimental section

2.1. Material processing

A screen printable thermoelectric paste basically contains 3 parts: fillers, epoxy binder system and solvent. In this experiment, the fillers were the thermoelectric material $\text{Bi}_{1.8}\text{Te}_{3.2}$ and Sb_2Te_3 particles with the size of 325 mesh and a purity of 99.99%. The particles were from Testbourne Ltd. The adjacent particles are stuck to each other and adhered onto the substrate by the epoxy binder system. The solvent was added into the paste to adjust the viscosity to a screen printable level. Finally, the paste was uniformly mixed by an EXAKT 50 triple roll mill. The viscosity of the pastes was in the range from 9000 cP to 15000 cP, measured by a Brookfield High Shear Cap-1000+ viscometer.

Initially, square thick film samples with dimensions of 1 cm \times 1 cm were printed in order to measure the effect of pressure on the Seebeck coefficient and resistivity. For the CIP process, first the pastes were fully dried after printing. Then the samples were put into plastic bags, coving with a silicone film on top of the patterns. The low surface energy of silicone can prevent the uncured paste from sticking onto the plastic bag [7]. After pressing, the samples were cured under 250°C for 3 hours. The CIP machine used was CIP-20TA from MTL.

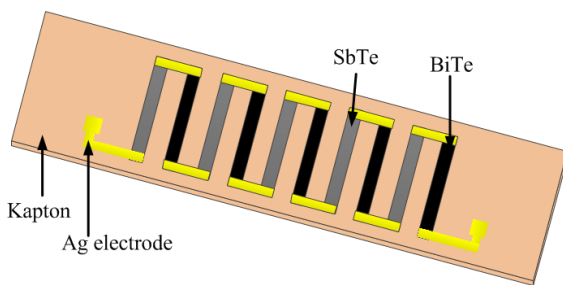


Figure 2. Illustration of screen printed planar-structured BiTe/SbTe TEGs.

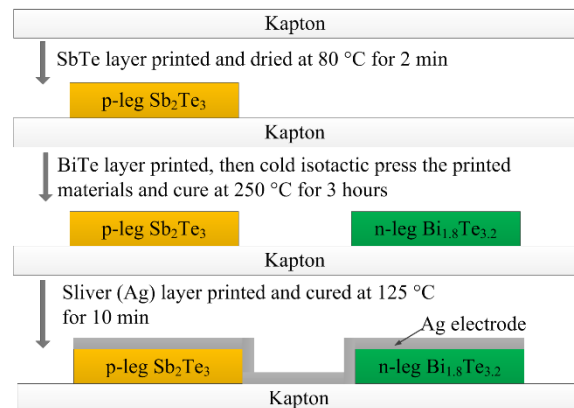


Figure 3. Fabrication process of screen printed TEGs.

2.2. Device fabrication and measurement

The schematic of the printed planar TEG was illustrated in figure 2. The thermocouples were connected electrically in series and thermally in parallel. A silver (Ag) thick film was printed on top of the thermocouples to act as electrodes. The size of an individual thermoleg was 20 mm \times 2 mm \times 78.4 μm (length, width and thickness) while the gap between adjacent thermolegs was 1 mm.

In order to realize this structure, a fabrication process shown in figure 3 was used. For this experiment, the volume of the CIP chamber limited the test structure to 8 thermocouples.

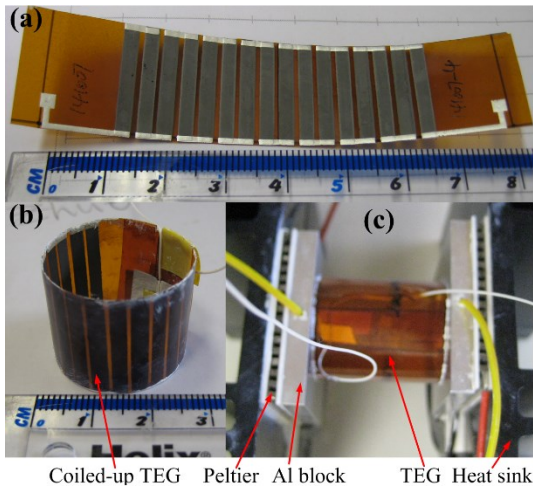


Figure 4. (a): Screen printed BiTe/SbTe TEG with Ag electrodes. (b): The coiled-up state of the TEG. (c): The setup to measure the generated thermoelectric voltage and power output when with load resistor

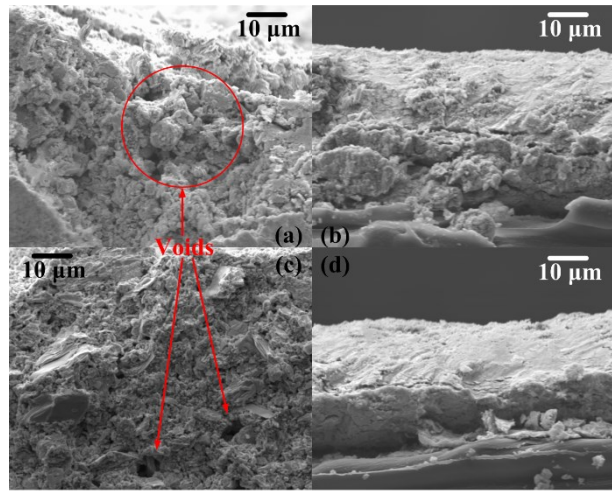


Figure 5. Cross-section SEM images of printed thermoelectric thick films. (a): BiTe thick film without pressing. (b): BiTe thick film with pressing. (c): SbTe thick film without pressing. (d): SbTe thick film with pressing.

The image of the screen printed planar TEG is shown in figure 4-(a). The strip can be rolled to a coil with a diameter of 2 cm (figure 4-(b)). In figure 4-(c), peltiers were used to supply the temperature gradient. Two square aluminum blocks were placed on the surface of each Peltier.

For the Seebeck coefficients measurement of individual materials, a bespoke test rig was used. The resistivity was measured through the Hall Effect measurement, using a commercial Hall Effect measurement system (HMS 3000 from Ecopia). The surface metrology of the samples was measured by the KLA-Tencor surface profiler.

3. Results and discussion

3.1. Material Properties

Compared with the samples without press by CIP, the pressed BiTe and SbTe thick films have a smaller surface roughness. The average distance between the highest peak and lowest valley in each sampling length is defined as a parameter (R_{tm}) and used as the measure of the surface roughness [8]. The difference of R_{tm} values for samples with and without pressing is shown in table 1. The R_{tm} values for both BiTe and SbTe thick films decreased by about 2 μm in average.

Table 1. R_{tm} values of BiTe and SbTe thick films with and without CIP.

	BiTe	SbTe
Without pressing	8000 nm	5500 nm
With pressing	6000 nm	3500 nm

Also, from the cross-section SEM images of the thick films with and without CIP in figure 5, it is observed that there were more voids in the un-pressed samples than the pressed ones. The decrease in voids created a denser film with improved electrical contact between adjacent particles. Therefore, the resistivity decreased with the densification of the thick film.

After the CIP process with an applied pressure of 250 MPa for 3 minutes, there was a reduction of 67% and 72% in resistivity compared with that of the sample without pressing for BiTe and SbTe thick films respectively. For both materials, higher CIP pressure leads to a lower resistivity. However, the

variation in Seebeck coefficients for both the BiTe and SbTe under different pressure are within 5% (figure 7). The Seebeck coefficient of BiTe/SbTe thermocouple was around 248 $\mu\text{V}/\text{K}$ calculated from the values after 250 MPa pressing.

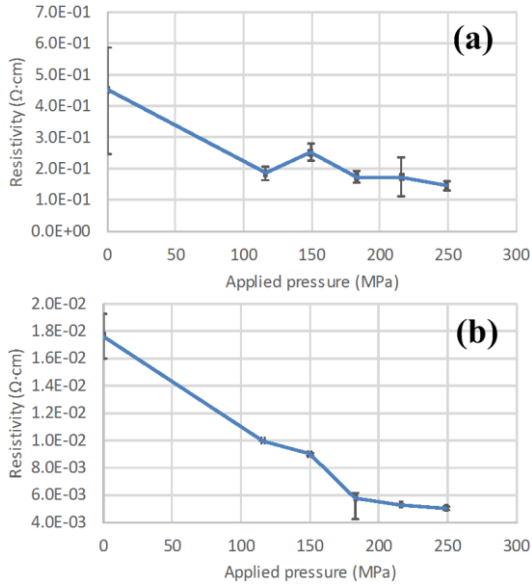


Figure 6. Electrical resistivity changing versus applied CIP pressure. (a): BiTe. (b): SbTe.

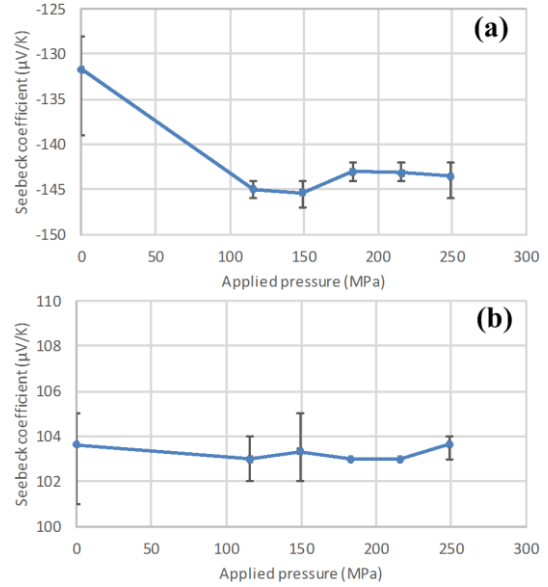


Figure 7. Seebeck coefficient changing versus applied CIP pressure. (a): BiTe. (b): SbTe.

3.2. Optimization of The Printing Process

In principle, the Ag connections can be either printed below or above the thermocouples. However, when Ag was printed as the bottom electrodes, the contact resistance between the Ag and the thermoelectric materials became unacceptably high. Table 2 lists the contact resistances between the Ag electrode and two adjacent thermolegs. The 15 junctions in figure 4-(a) had an average contact resistance of 1.3 k Ω , which is 300 times lower than the sample using Ag as bottom electrodes. Therefore, top electrodes were used in the fully screen printed Flexibly TEG.

Table 2. The resistance of single junction of BiTe/SbTe when use Ag as bottom and top electrodes

	Ag on bottom	Ag on top
Range	3.0 k Ω ~ 2.6 M Ω	0.3 k Ω ~ 2.3 k Ω
Average	437 k Ω	1.3 k Ω

3.3. Device Performance

At a temperature gradient (ΔT) of 20 $^{\circ}\text{C}$, the fully screen printed TEG generated a voltage of 36.4 mV. In figure 8, the voltage shows a linear relationship with the temperature gradient. The Seebeck coefficient of single thermocouple can be calculated out to be 227 $\mu\text{V}/\text{K}$ based on the definition of the Seebeck Effect ($V=n\cdot\alpha\cdot\Delta T$, V is the open circuit voltage and n is the number of thermocouples) [1].

From figure 9, the maximum power output when $\Delta T=20^{\circ}\text{C}$ was 40.3 nW. The contact resistance contributed most of the device resistance, which limited the power output. The coiled-up TEG had a resistance of 7.2 k Ω including the contact resistance. A possible reason for the high contact resistance is the formation of an insulating layer at the interface due to chemical incompatibility.

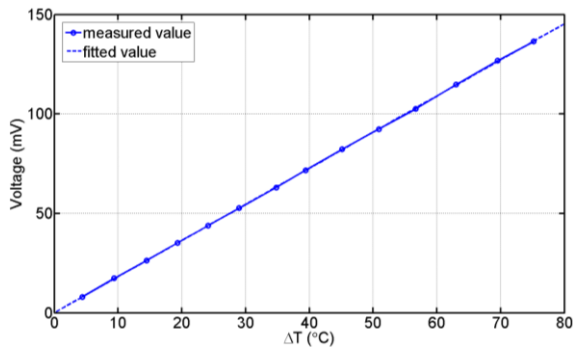


Figure 8. Generated Seebeck voltage of the coiled-up TEG at different temperature gradient

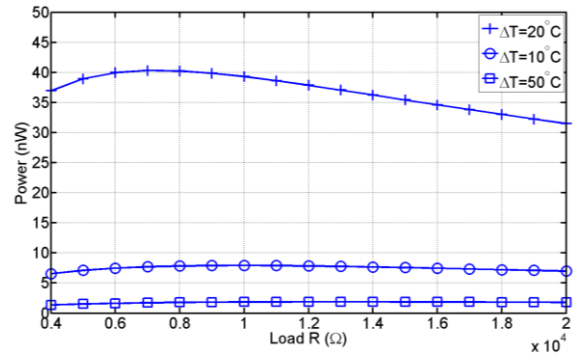


Figure 9. Power output of the coiled-up TEG varies with load resistance

4. Conclusion

The CIP process has been demonstrated to decrease the resistivity of the thick films by densifying the materials. For SbTe thick film, the lowest resistivity measured in this experiment was $5.01 \times 10^{-3} \Omega \cdot \text{cm}$, which is lower than the value of $2.0 \times 10^{-2} \Omega \cdot \text{cm}$ reported in the literature [9]. However, the resistivity of BiTe thick film was still high and needs further investigation.

On the device level, a fully screen printed flexible TEG with Ag electrode connections was fabricated and tested. The Ag films were optimized to be printed as top electrodes rather than bottom electrodes. However, the contact resistance was still too high and limits the power output. In future work, approaches to reduce the contact resistance will be investigated.

5. Acknowledgements

The authors thank the EPSRC for supporting this research with grant reference EP/I005323/1. We would also like to thank Kai Yang, Yi Li and Luyi Yang for their contributions.

References

- [1] S. Beeby and N. White 2010 *Energy Harvesting for Autonomous Systems*. (Norwood, MA: Artech House)
- [2] S. L. Kim, K. Choi, A. Tazebay, and C. Yu 2014 *ACS Nano*, **8**, 3, 2377–86
- [3] V. Leonov 2011 *ISRN Renew. Energy* **2011** 1–11
- [4] Z. Cao, E. Koukharenko, M. J. Tudor, R. N. Torah, and S. P. Beeby 2013 *J. Phys. Conf. Ser.* **476** 012031
- [5] W. Glatz and C. Hierold 2007 *Micro Electro Mechanical Systems, 2007. MEMS. IEEE 20th International Conference on (Hyogo, Japan, 21-25 Jan. 2007)* pp. 89-92
- [6] M. Koizumi and M. Nishihara 1991 *Isostatic Pressing: Technology and Applications* (Barking, England: Springer Science & Business Media)
- [7] C. Wetzel, J. Schönfelder, W. Schwarz, and R. H. W. Funk 2010 *Surf. Coatings Technol.* **205** 1618–1623
- [8] A. N. S. Institute and A. S. o. M. Engineers 1996 *Surface Texture Symbols: ASME Y14.36M-1996* (New York: American Society of Mechanical Engineers)
- [9] A. Chen, D. Madan, P. K. Wright, and J. W. Evans 2011 *J. Micromechanics Microengineering* **21** 104006